(4)

MARYLAND

COLLEGE PARK CAMPUS

THE P-VERSION OF THE FINITE ELEMENT METHOD FOR DOMAINS WITH CORNERS AND FOR INFINITE DOMAINS

by

IVO BABUŠKA *
INSTITUTE OF PHYSICAL SCIENCE AND TECHNOLOGY
UNIVERSITY OF MARYLAND
COLLEGE PARK, MARYLAND 20742

and

HAE-SOO OH
DEPARTMENT OF MATHEMATICS
UNIVERSITY OF NORTH CAROLINA AT CHARLOTTE
CHARLOTTE, NORTH CAROLINA 28223

BN-1091

November 1988

INSTITUTE FOR PHYSICAL SCIENCE AND TECHNOLOGY

SECURITY CLASSIFICATION OF THIS PAGE (When Data Entered)

REPORT DOCUMENTATION PAGE

READ INSTRUCTIONS BEFORE COMPLETING FORM

1. REPORT NUMBER: BN-1091	2. GOVT ACCESSION NO.
3. RECIPIENT'S CATALOG NUMBER	
4. TITLE (and Subtitle): The p-Version of the Finite Element Method for Domains with Corners and for Infinite Domains	5. TYPE OF REPORT & PERIOD COVERED: Final life of contract
6. PERFORMING ORG. REPORT NUMBER	
7. AUTHOR(s): I. Babuska[1] and Hae-Soo Oh	8. CONTRACT OR GRANT NUMBER(s): [1]ONR N00014-85-K-0169; NSF DMS-85-60191
9. PERFORMING ORGANIZATION NAME AND ADDRESS: Institute of Physical Science and Technology, University of Maryland, College Park, MD 20742	10. PROGRAM ELEMENT, PROJECT, TASK AREA & WORK UNIT NUMBERS
11. CONTROLLING OFFICE NAME AND ADDRESS: Department of the Navy, Office of Naval Research, Arlington, VA 22237	12. REPORT DATE: November 1988
	13. NUMBER OF PAGES: 39
14. MONITORING AGENCY NAME & ADDRESS (if different from Controlling Office)	15. SECURITY CLASS. (of this report)
	15a. DECLASSIFICATION/DOWNGRADING SCHEDULE

16. DISTRIBUTION STATEMENT (of this Report)

Approved for public release: distribution unlimited

17. DISTRIBUTION STATEMENT (of the abstract entered in Block 20, if different from Report)

18. SUPPLEMENTARY NOTES

19. KEY WORDS (Continue on reverse side if necessary and identify by block number)

20. ABSTRACT (Continue on reverse side if necessary and identify by block number)

A special approach to deal with elliptic problems with singularities is introduced. It is shown that this approach, to be called the auxiliary mapping technique, in the frame of the p-version of the finite element method yields an exponential rate of convergence at virtually no extra cost and from the view-point of implementation it is the easiest and the cheapest method of all. It also shown that this technique can be used for elliptic problems on unbounded domains in R^2 as well.

DD FORM 1 JAN 73 1473 EDITION OF 1 NOV 65 IS OBSOLETE

S/N 0102-LF-014-6601

SECURITY CLASSIFICATION OF THIS PAGE (When Data Entered)

THE P-VERSION OF THE FINITE ELEMENT METHOD FOR DOMAINS WITH CORNERS AND FOR INFINITE DOMAINS

by

IVO BABUŠKA *
INSTITUTE OF PHYSICAL SCIENCE AND TECHNOLOGY
UNIVERSITY OF MARYLAND
COLLEGE PARK, MARYLAND 20742

and

HAE-SOO OH
DEPARTMENT OF MATHEMATICS
UNIVERSITY OF NORTH CAROLINA AT CHARLOTTE
CHARLOTTE, NORTH CAROLINA 28223

*Partially supported by the Office of National Research under Contract N00014-85-K-0169 and by the National Science Foundation under Grant DMS-85-16191.

THE P-VERSION OF THE FINITE ELEMENT METHOD FOR DOMAINS WITH CORNERS AND FOR INFINITE DOMAINS

by

IVO BABUŠKA
INSTITUTE OF PHYSICAL SCIENCE AND TECHNOLOGY
UNIVERSITY OF MARYLAND
COLLEGE PARK, MARYLAND 20742

and

HAE-SOO OH
DEPARTMENT OF MATHEMATICS
UNIVERSITY OF NORTH CAROLINA AT CHARLOTTE
CHARLOTTE, NORTH CAROLINA 28223

Abstract. A special approach to deal with elliptic problems with singularities is introduced. It is shown that this approach, to be called **the auxiliary mapping technique**, in the frame of the p-version of the finite element method yields an exponential rate of convergence at virtually no extra cost and from the view-point of implementation it is the easist and the cheapest method of all. It is also shown that this technique can be used for elliptic problems on unbounded domains in R^2 as well.

AMS(MOS) Subject Classifications. Primary 65N30, 65N15

Key Words: Auxiliary Mapping Technique, The p-Version of the Finite Element Method, Domains with Corners, Unbounded Domains, Circular Arc Property, Conforming Element.

1. Introduction

In the theory and practice of the finite elements a considerable effort has been made to design special approaches to deal with problems on domains with corners (especially, cracks) and with problems on infinite domains.

In the case of nonsmooth boundaries the following approaches are the most typical:

($1A$) Mesh Refinement([4],[6],[7],[8],[9],[13],[14],[25]).

($1B$) Use of Special Elements([1],[2],[22],[26]).

($1C$) Use of the Enriched (nonlocal) Bases Functions([16],[23]).

In the case of the infinite domains, the widely used approaches are:

($2A$) Domain Restriction Procedure([15],[17]).

($2B$) The Boundary Element Method and Combination of the Finite Element Method and the Boundary Element Method([18],[21]).

($2C$) Infinite Element Approach([28],[29]).

The method ($1C$) is in practice almost never used because this approach destroys the architecture of the finite element method program. The method ($1B$) is to devise special finite elements in which the approximation mimics the singularity in elements neighboring singular points. By this the accuracy is increased, nevertheless the rate of convergence of the h-version is not improved. By far the most effective approach for handling singularities is the method ($1A$) but the success of it depends on the proper mesh refinement.

The method ($2C$) is not often used in practice. The Boundary Element Method handles well the problem with constant coefficients on domains with bounded boundary, but this method has difficulties when the coefficients of the equation are not constant, the boundary is unbounded, and is ineffective when the differential equation is not homogeneous. The hybrid method between the Finite Element Method and the Boundary Element Method is sometimes used but lies in the h-version and it has the same character and difficulty

as $(1B)$. The most widely used method in practice for dealing with infinite domain is the method $(2A)$. However the main concern in this approach is to choose the truncating domain properly to get a desired accuracy.

There are three versions of the finite element method: the h- version, the p-version, and the h-p version. The h-version is the standard one, where the degree p of the elements is fixed, usually on low level, typically $p = 1, 2, 3$ and the accuracy is achieved by properly refining the mesh. The p-version, in contrast, fixes the mesh and achieved the accuracy by increasing the degrees p of the elements uniformly or selectively. The h-p version is the combination of both. In this paper, we are mainly concerned with the p-version of the finite element method([8],[10]). We will see that the p-version in many cases avoids naturally some difficulties arising in the h-version because it uses elements of large size.

The basic aspects of the finite element approach are

(a) The geometry, where the domain is defined and partitioned into elements.

(b) Creation of elemental stiffness matrices and elemental load vectors.

(c) Assembling elemental stiffness matrices and load vectors together to form the global stiffness matrix A and the global load vector b

(d) Solving the system $Ax = b$

(e) Post processing.

The elemental stiffness matrices are based on the (elemental) mapping of the element onto the standard element and the polynomial shape functions on the standard element. The usual (elemental) mapping is typically of isoparametric or blending type.

In this paper, addressing two dimensional problems, we will show that the effective use of other mapping (for example conformal mapping or quasi conformal mapping) in conjunction with the usual (elemental) mapping in the frame of the p-version of the finite element method yields an exponential rate of convergence at virtually no extra cost. This approach can be directly and practically, without any changes, implemented in the p-version of the Finite Element Code PROBE([24]).

The outline of this paper is as follows: In section 2 the generalized elements are introduced and the conditions for elemental mappings to yield conforming elements are stated. Also listed are some preliminary lemmas. In section 3 we prove that the p-version of the finite element method leads to an exponential rate of convergence when the exact solution of the problem is analytic. In section 4 the method of auxiliary mappings is introduced. It is shown that one can obtain an exponential rate of convergence at no extra cost when this technique is applied to Laplace equations on domains with corners. In section 5 we show that the mapping technique also works for general elliptic boundary value problems. In section 6 this technique is applied to the problems on the exterior of the bounded domains. Finally, the conclusions are summarized in section 7.

2. Preliminaries

Throughout this paper, Ω denotes a simply connected (bounded or unbounded) open subset of R^2 , where R^2 denotes the usual Euclidean space with $x = (x_1, x_2) \in R^2$. As we mentioned above, the domain Ω under consideration is partitioned into the elements $e_i, i = 1, 2, ...n$. By an *element* e we mean an open curvilinear triangle or rectangle. A curvilinear triangle is a domain which is bounded by three smooth(analytic) arcs(sides) whose ends are called the vertices. A curvilinear rectangle has analogous meaning. We allow the triangle to be unbounded, where one vertex is located at ∞ analogously as in the theory of complex variable. Then $\overline{\Omega} = \cup_i \overline{e_i}$, where by the bar we mean the closure in R^2 . As usual, we will assume that $e_i \cap e_j$ is either empty or is a common vertex or is an entire common side.

By T and Q we denote the standard triangular element and the standard quadrilateral element respectively as shown in Fig.2.1$(a)(b)$. The coordinates in the standard plane are denoted by $\xi = (\xi_1, \xi_2)$. As usual we define on the element e the finite element space $S(e)$

which is the span of elemental shape functions, denoted by $N_i^e(x), x \in e$, i.e. $S(e) = \text{span}_i N_i^e(x)$.

By the standard shape function $\mathcal{N}_i(\xi)$ we mean the shape functions on the standard element $E(E = T \text{ or } E = Q)$ which are divided into the groups of (1) nodal, (2) side and (3) internal shape functions. We assume as usual that a bijective smooth elemental mapping Φ_e from E to e is such that $\Phi_e(\xi) = x \in e$, for $\xi \in E$, where $E = T$ or $E = Q$ according as e is (curvilinear) triangular element or (curvilinear) quadrilateral element.

Then the elemental shape functions N_i^e are related to the standard shape function by $N_i^e(x) = \mathcal{N}_i(\Phi_e^{-1}(x))$(equivalently by $N_i^e(\Phi_e(\xi)) = \mathcal{N}_i(\xi)$). Alternatively we denote it by $N_i^e = \mathcal{N}_i \circ \Phi_e^{-1}$(or $\mathcal{N}_i = N_i^e \circ \Phi_e$). We associated to every element e_i of the partition of Ω the mapping Φ_{e_i}. We will assume that these mappings satisfy the usual conditions used in the finite element method that lead to conforming finite elements. This means that if A is a common vertex of the element e_{k_j} , $j = 1, 2, ...m$ and $N_{i_j}^{e_{k_j}}$ are the nodal shape functions associated to the vertex A then the function v such that

$$\begin{cases} v(x) & = N_{i_j}^{e_{k_j}}(x) \quad \text{on } e_{k_j}, j = 1, 2, ..., m \\ v(x) & = 0 \qquad \text{for } x \notin e_{k_j}, j = 1, 2, ...m \end{cases}$$

is a continuous function on Ω . Similarly if γ is the common side of elements e_{k_1} and e_{k_2} and

$$N_{i_j}^{e_{k_j}}, j = 1, 2$$

are the side shape functions associated to the common side then the function v defined by

$$\begin{cases} v(x) & = N_{i_j}^{e_{k_j}}(x) \quad \text{on } e_{k_j}, j = 1, 2. \\ v(x) & = 0 \qquad \text{for } x \notin e_{k_j}, j = 1, 2. \end{cases}$$

is a continuous function on Ω . Finally the supports of the internal shape functions are in the element.

There are many possible elemental mappings. We will impose some restriction on the elemental mappings. Especially we will assume that Φ_e has *the circular arc property:* Let e be a curvilinear triangle with a circular side as shown in Fig. 2.2, then Φ_e linearly transforms the length of *arc* of the standard triangle on the length of *arc* of the element e. If e is a curvilinear quadrilateral element with a circular side, the meaning of Φ_e with circular property is analogous. Let us note that the code PROBE([24]) is using the elemental mappings with circular arc property.

In general we will consider two domains Ω and $\hat{\Omega}$ in R^2 such that $\Psi(\Omega) = \hat{\Omega}$ where Ψ is a smooth bijective mapping of Ω onto $\hat{\Omega}$. If u is a funtion defined on Ω then $\hat{u}$ will denote the function defined on $\hat{\Omega}$ by

$$\hat{u} = u \circ \Psi^{-1}(\text{ or } u = \hat{u} \circ \Psi)$$

Obviously if $\Omega = e, \hat{\Omega} = T(\text{ or } Q)$ then $\Psi = \Phi_e^{-1}$ as a special case of notation we have used above. When there is a mapping φ which transforms a curvilinear triangular (quadrilateral) element e onto an element e^* of the same type, we will construct the elemental mapping Φ_{e^*} of the standard element $E(E = T \text{ or } Q)$ onto e^* so that

$$\begin{aligned} \mathcal{N}_i \circ \Phi_{e^*}^{-1} = N_i^{e^*} &= (N_i^e) \circ \varphi^{-1} \\ &= \mathcal{N}_i \circ \Phi_e^{-1} \circ \varphi^{-1} \quad \text{for any shape function } \mathcal{N}_i \text{ on } E. \end{aligned}$$

Note that if φ^{-1} is a mapping, from an element e^* with a circular side onto another element e with a circular side, which is linear in the arc-length, and if Φ_{e^*} has circular arc property then the composite mapping $\varphi^{-1} \circ \Phi_{e^*}$ also has the circular arc property. We have seen that the main objective is to create the set $S(e)$ of elemental shape functions which led to the conforming base functions. We can now use not only one elemental mapping but a family of such mappings. For example, let $\tilde{\varphi}^{-1}$ maps $\tilde{e}^*$, an element with circular side,onto e , an element with circular side, then we can enrich the space of elemental shape functions for e by functions $\mathcal{N}_i \circ \Phi_{\tilde{e}^*}^{-1} \circ \tilde{\varphi}$, where $\mathcal{N}_i$ denotes the standard shape functions which are

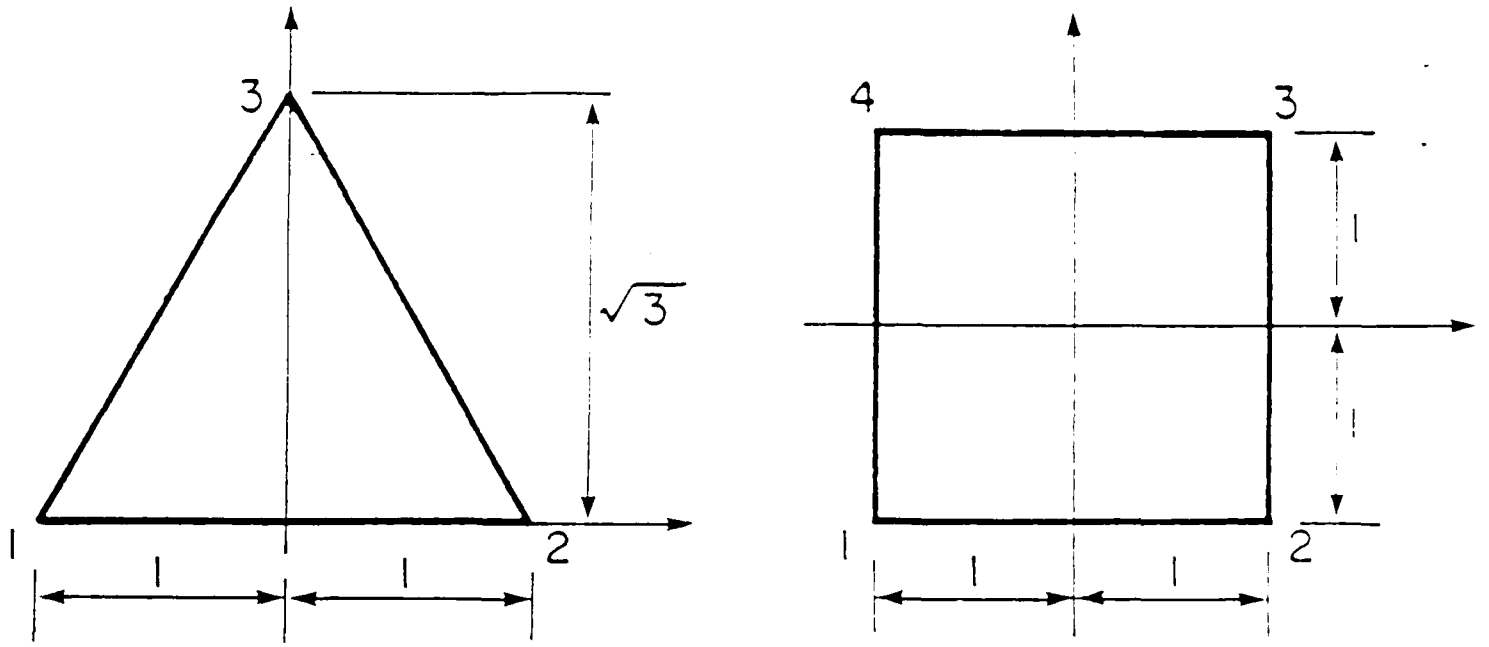

Fig. 2.1. (a) The Standard Triangular Element. (b) The Standard Quadrilatral Element.

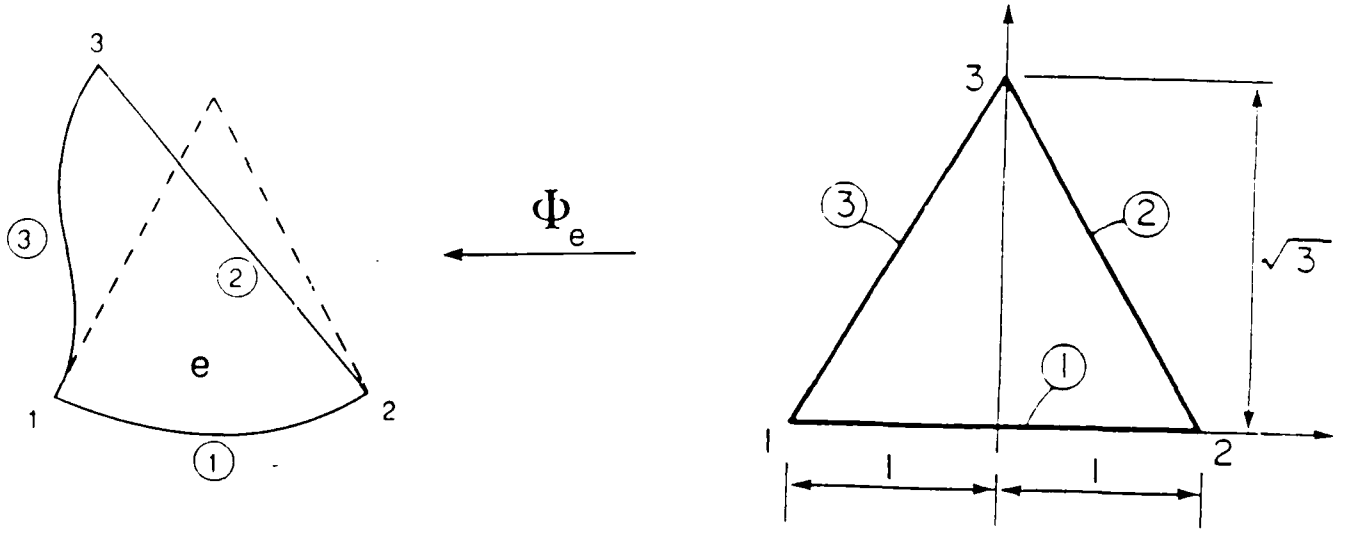

Fig. 2.2. An Elemental Mapping Φ_e of the Standard Triangular Element T onto a Curvilinear Tringular Element e.

zero on the side of the standard element that is not associated to the circular side. So far we mentioned only the objective to construct the elemental shape functions. The next objective is to construct them so that local stiffness matrices can be easily computed.

Returning now to the general mapping Ψ of Ω onto $\hat{\Omega}$, we denote the Jacobian of Ψ^{-1} by $J(\Psi^{-1})$ and its determinant by $|J(\Psi^{-1})|$ and we will assume it is positive on $\hat{\Omega}$. Then we define

$$M = (|J(\Psi^{-1})|)^{1/2}(J(\Psi) \circ \Psi^{-1})$$

and we get an obvious lemma.

Lemma 2.1. *Suppose* $A = [a_{ij}], a_{ij} \in L_\infty(\Omega), 1 \leq i,j \leq 2$ *and if* $Q = M\{a_{ij} \circ \Psi^{-1}\}M^T = \{q_{ij}\}$, *then we get*

$$\iint_\Omega \sum a_{ij}(x)\frac{\partial u}{\partial x_i}\frac{\partial v}{\partial x_j} = \iint_{\hat{\Omega}} \sum q_{kl}(\xi)\frac{\partial \hat{u}}{\partial \xi_k}\frac{\partial \hat{v}}{\partial \xi_l} \tag{2.1}$$

and $q_{kl}(\xi) \in L_\infty(\hat{\Omega})$.

We are particularly interested in the special case when $A = I$,the identity matrix and Ψ is a conformal mapping of Ω onto $\hat{\Omega}$. Then we have

Corollary 2.1. *If* Ψ *is a conformal mapping and* $A = I$ *then* $Q = I$, *that is,*

$$\iint_\Omega \nabla u \cdot \nabla v dx = \iint_{\hat{\Omega}} \nabla \hat{u} \cdot \nabla \hat{v} d\xi.$$

Corollary 2.2. *Let* $A = \{a_{ij}(x)\}$ *be a symmetric* 2×2 *matrix such that*

$$|a_{ij}(x)| < \gamma_1 < \infty, \quad \sum a_{ij}(x)\eta_i\eta_j \geq \gamma_2(\eta_1^2 + \eta_2^2), \gamma_2 > 0,$$

for all $(\eta_1, \eta_2) \in R^2$ *and if* Ψ *is a conformal mapping, then we have*

$$q_{kl}(\xi) < \gamma_1^* < \infty, \quad \sum q_{kl}(\xi)\eta_k\eta_l \geq \gamma_2^*(\eta_1^2 + \eta_2^2), \gamma_2^* > 0,$$

for any $(\eta_1, \eta_2) \in R^2$, *where* γ_1^* *and* γ_2^* *depend on the mapping but not on* ξ . *Hence the conformal mapping preserves the ellipticity of the operator*

$$L = \sum \frac{\partial}{\partial x_i}(a_{ij}(x)\frac{\partial}{\partial x_j}).$$

Let us note that Corollary 2.2 is also true under a weaker condition on Ψ , for example, when

$$J(\Psi)J(\Psi)^T = |J(\Psi)|\text{diag}(d_1(x), d_2(x))$$

and

$$0 < k_1 \leq d_i(x) \leq k_2, \text{ for all } x \in \Omega.$$

Finally we would like to mention a conformal mapping which will play an important role in forthcomming sections:

$$z = \xi^\alpha, \quad z = x_1 + ix_2, (x_1, x_2) \in e(\text{ resp } \Omega)$$

$$\xi = \xi_1 + i\xi_2, (\xi_1, \xi_2) \in e^*(\text{ resp } \hat{\Omega})$$

and this mapping characterized by the constant α will be denoted by φ^α (resp Ψ^α) respectively.

3. The p-Version of the Finite Element Method

Let $\Omega \subseteq R^2$ be a bounded domain whose boundary Γ is composed of smooth (analytic) arcs Γ_i, i.e. $\Gamma = \cup_i \Gamma_i$.

Consider now the following model problem

$$-\Delta u = f \quad \text{in } \Omega, \tag{3.1a}$$

$$u = 0 \quad \text{on } \Gamma_D = \cup_{i \in \mathcal{D}} \Gamma_i, \tag{3.1b}$$

$$\frac{\partial u}{\partial n} = g \quad \text{on } \Gamma_N = \cup_{i \in \mathcal{N}} \Gamma_i, \tag{3.1c}$$

where $\mathcal{D} \cap \mathcal{N} = \phi, \Gamma_N \cup \Gamma_D = \Gamma$, and $g \in L_2(\Gamma_N)$. For simplicity we assume that $\Gamma_D \neq \phi$ (otherwise the solution would not be unique and we would have to use the standard approach which would avoid this technical difficulty).

Let $H^1(\Omega)$ be the usual Sobolev space and $H^1_D = \left\{u \in H^1(\Omega) : u = 0 \text{ on } \Gamma_D\right\}$ then as usual we will consider the weak solution of the problem: Find $u_0 \in H^1_D(\Omega)$ such that

$$B(u_0, v) = F(v), \text{ for all } v \in H^1_D(\Omega)$$

where

$$B(u, v) = \iint_\Omega \nabla u \cdot \nabla v dx,$$

$$F(v) = \iint_\Omega f v dx + \int_{\Gamma_N} g v ds.$$

Furthermore we denote $\|u\|^2_E = B(u, u)$ and will call $\|.\|_E$ energy norm. Because of the assumption on Γ_D we have $\|u\|_E = \|u\|_{H^1(\Omega)}$.

Let us now consider a (fixed) partitioning of Ω into the elements e_i, i.e. $\overline{\Omega} = \cup \overline{e_i}$ as in the previous sections. Because of the assumption about e, the vertices of Ω are the vertices of some elements. We will assume that the partition and the (elemental) mapping

Φ_e introduced in the previous section satisfy the (technical) conditions listed in ([4], [14]) that are satisfied in the code PROBE.

Let

$$S_p = \{u \in H_D^1(\Omega) : u|_e \circ \Phi_e \text{ is a polynomial of degree } p \text{ on } E \text{ for all element } e\},$$

where E is T or Q according as e is a triangular element or a rectangular element, and let N_p be the dimension of S_p. Then the p-version of the finite element method is now to find $u_p \in S_p$ such that

$$B(u_p, v) = F(v), \text{for all } v \in S_p$$

and then

$$\|u_p - u_0\|_E = \min_{w \in S_p} \|w - u_0\|_E. \tag{3.2}$$

We have now

Theorem 3.1. *Let $u_0 \in H_D^1(\Omega)$ be such that*

$$\|u_0\|_{H^k(\Omega)} \leq C D^k k!, k = 1, 2, ... \tag{3.3}$$

where $H^k(\Omega)$ is the usual Sobolev space and C and D are constants independent of k, then

$$\|u_0 - u_p\|_E \leq C e^{-\gamma\sqrt{N_p}} \tag{3.4}$$

where c and $\gamma > 0$ are independent of p.

Proof. By modifying the proof given in [4], one can easily proceed the proof of this theorem. Hence we will only outline the key steps of the proof.

(i) Denoting $u_e = u|_e$ the restriction of u on the element e, we define $\hat{u}_e = u_e \circ \Phi_e$, where Φ_e is the elemental mapping of the standard element E onto e.

(ii) We construct $\hat{u}_{e,p} \in H^1(E)$ which is a polynomial of degree p on E and approximates the function $\hat{u}_e$ in $H^1(E)$. Using (3.3) we get

$$\|\hat{u}_e - \hat{u}_{e,p}\|_{H^1(E)} \leq Ce^{-\gamma_1 p} \tag{3.5}$$

(iii) Let $\bar{u}_{e,p} = \hat{u}_{e,p} \circ \Phi_e^{-1}$, then $\hat{u}_{e,p}$ approximates u_e on e and satisfies

$$\|u_e - \bar{u}_{e,p}\|_{H^1(e)} \leq C_1 e^{-\gamma_2 p}$$

but $\bar{u}_{e,p} \notin H_D^1(\Omega)$

(iv) We construct a correction term on every e so that the correction function u_p can be a member of $H_D^1(\Omega)$ and satisfy (3.4). **(QED)**

We also have

Theorem 3.2. *Let Ω be a polygonal domain and if $u_0 \in H^q(\Omega)$, $q > 1$ integer or fractional, then we have*

$$\|u_0 - u_p\|_E \leq CN_p^{-(q-1)/2}\|u_0\|_{H^q(\Omega)}$$

If $u_0 = cr^\beta \varphi(\theta)\chi(r,\theta)$, where (r,θ) are the polar coordinates at the vertex A of Ω ,$\varphi(\theta)$ is a smooth function and $\chi(r,\theta)$ is a smooth cut-off function, then

$$\|u_0 - u_p\|_E \leq CN_p^{-\beta}$$

For the proof, see [8]. **(QED)**

Example 3.1 Let Ω be an L-shaped domain partitioned into 12 elements as shown in Fig. 3.1 and

$$\mathcal{D} = \{1, 2\}$$

$$\mathcal{N} = \{3, 4, 5, 6, 7, 8\}$$

$$g = 1 \text{ on } \Gamma_i, i = 4, 5, 6, 7$$

$$g = 0 \text{ on } \Gamma_i, i = 3, 8$$

Let us assume $f = 0$ and Ω_{R_0} denotes the circular subset of Ω which is composed of the curved triangular elements in Fig 3.1. Then on $\tilde{\Omega} = \Omega - \Omega_{R_0}$ the solution u_0 satisfies (3.3), but on Ω it only satisfies $u_0 \in H^{5/3-\epsilon}(\Omega)$, where ϵ is an arbitrary positive number. Moreover the solution has the leading term $r^{2/3}\sin(2/3)\theta$ near the re-entrant corner.

Hence applying theorem 3.2 we get

$$\varepsilon_0(p) = \frac{\|u_0 - u_p\|_E}{\|u_0\|_E} \leq C N_p^{-2/3}$$

Fig. 4.2 shows ε_0 in dependence on N_p in $\log \times \log$ scale. It also shows the slope of the rate $N_p^{-2/3}$. If we would solve the problem on $\tilde{\Omega}$ then we would get

$$\|u_0 - u_p\|_E \leq C e^{-\gamma\sqrt{N_p}}$$

that is, the exponential rate. Hence we see that the error decrease algebraically only because the function from S_p are not able to approximate well the solution in Ω_{R_0}.

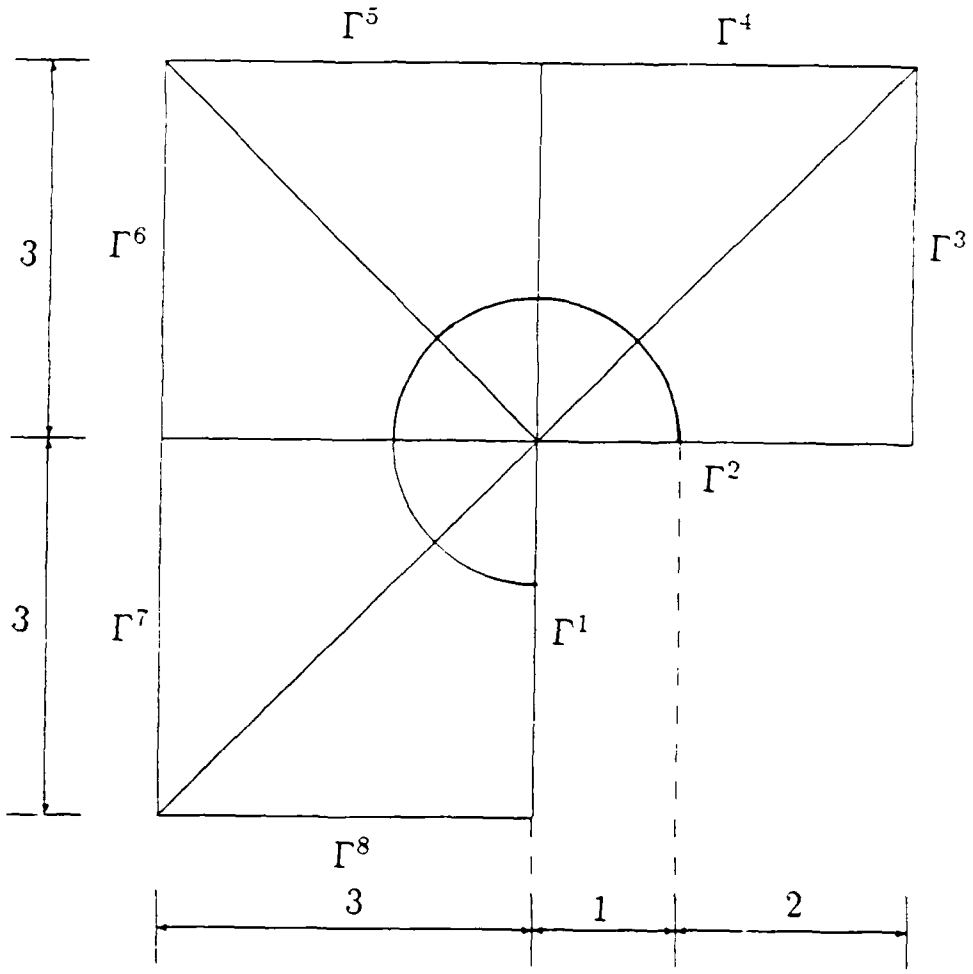

Fig. 3.1. The Scheme of the L-Shaped Domain Ω and a Subdomain Ω_{R_0}.

4. The Method of Auxiliary Mapping for the Laplace Operator.

So far we constructed the spaces $S(e)$ by using the standard elemental mappings Φ_e which were based on the blending mapping technique.

Let us now propose the question about optimal mapping technique which is adjusted according to the character of the solution. To each element e we associate a mapping φ_e (see Section 2) which maps e onto $e^* = \varphi_e(e)$, and then use the composite mapping

$$\Phi_e = (\varphi_e)^{-1} \circ \Phi_{e^*}$$

for constructing $S(e)$. We will say that the set of mappings φ_e is *admissible* if the mappings $\{(\varphi_e)^{-1} \circ \Phi_{e^*}\}$ will lead to conforming elements (see Section 2). Now the problem is following: Describe the families of admissible mappings and select one family that leads to optimal (in some sense) results.

Let us show such a family on the mesh shown in example 3.1. Let us map the element $e_j, j = 7,..,12$ (see Fig. 4.1) onto the element e_j^* by the conformal map $(\varphi^\alpha)^{-1}$, where $\varphi^\alpha : \xi^\alpha = z$. The mappings $\{(\varphi_j^\alpha)^{-1} : j = 7,...,12\}$ stemming from the conformal mapping $(\varphi^\alpha)^{-1}$, $\alpha \geq 3/2$ and the identity mappings $\varphi_i, i = 1,2,..6$, lead to the conforming elements. In fact (because $R_0 = 1$) the curvilinear triangles $e_j, j = 7,...,12$ are mapped by the mapping $(\varphi_j^\alpha)^{-1}$ onto the curvilinear triangle e_j^* and the mapping is linear on the circular arc. This together with the fact that Φ_{e^*} has the circular arc property shows that elements constructed by $\varphi^\alpha \circ \Phi_{e^*}$ are conforming. Using Corollary 2.1, we see that in our example the elemental stiffness matrices of $e_j, j = 7,...,12$ obtained by using the elemental mapping $\Phi_{e_j} = \varphi^\alpha \circ \Phi_{e_j^*}$ is identical with the elemental stiffness matrix of the element e_j^* obtained by using the element mapping $\Phi_{e_j^*}$. These stiffness matrices are directly computable, for example, by the code PROBE. The conformal mapping φ_j^α then has the obvious form: let (r,θ) be the polar coordinates in the z-plane and (ρ,ψ) the polar coordinates in the ξ-plane , then we have

$$r = \rho^\alpha \text{ and } \theta = \psi\alpha; \;\; \rho = r^{1/\alpha} \text{ and } \psi = \theta/\alpha$$

and if $e = \{(r,\theta)|0 < r < R_0, \beta_0 < \theta < \beta_1\}$ then $e^* = \{(\rho,\psi)|0 < r < R_0^{1/\alpha}, \beta_0/\alpha < \psi < \beta_1/\alpha\}$. Hence we compute the elemental stiffness matrix for e in e^* instead of in e, that is, in the ξ-plane.

Assume now that $f = 0$ in (3.1) then the exact solution u_0 can be written in the form of a series

$$u_0(r,\theta) = \sum_{k=1}^{\infty} a_k r^{(2/3)k} \sin(2/3)k\theta \text{ on } \Omega_{R_0} \tag{4.1}$$

The series converges absolutely on Ω_{R_0}. Now using the conformal mapping $\varphi^\alpha : z = \xi^\alpha$ we have $\hat{u}_0 = u_0 \circ \varphi^\alpha$ and

$$\hat{u}_0(\rho,\psi) = \sum_{k=1}^{\infty} a_k \rho^{(2/3)\alpha k} \sin(2/3)\psi k\alpha \text{ on } \Omega^*_{R_0}. \tag{4.2}$$

Hence if $\alpha = (3/2)m, m$ an integer, $\hat{u}_0$ is an analytic function. Using now this mapping in the finite element method we approximate the function $\hat{u}_0$ on e_j^* instead of the function u_0 on e_j. Denoting the finite element solution which is based on the elemental mapping $\varphi^\alpha \circ \Phi_{e_j^*}$ by u_p^α, we get

Theorem 4.1. *Let us consider the problem given in example 3.1 with $f = 0$. Suppose $\alpha = (3/2)m$, m is an integer. Then we get*

$$\|u_p^\alpha - u_0\|_E \leq Ce^{-\gamma\sqrt{N_p}}$$

where C and γ are independent of p (and hence N_p)

Proof.

$$\|u_p^\alpha - u_0\|_{H^1(e_j)} \leq C\|u_p^* - \hat{u}_0\|_{H^1(e_j^*)}$$

and apply theorem 3.1 with minor modification. **(QED)**

Tables 4.1 shows the relative errors for $m = 2/3, 1, 2$ and 4. Note that $m = 2/3$ means the case when no mapping technique was used. Figs. 4.2 and 4.3 show the error ε in $\log \varepsilon \times \log N$ scale and Fig. 4.4(a) shows the error in $\log \varepsilon \times \sqrt{N}$ scale.

We see the large improvement by this approach. The values $\alpha = m(3/2)$ is obviously the most advantageous in this case. Nevertheless for general $\alpha > 1, \alpha \neq m(3/2)$ we get an asymptotic improvement. By applying Theorem 3.2, we get

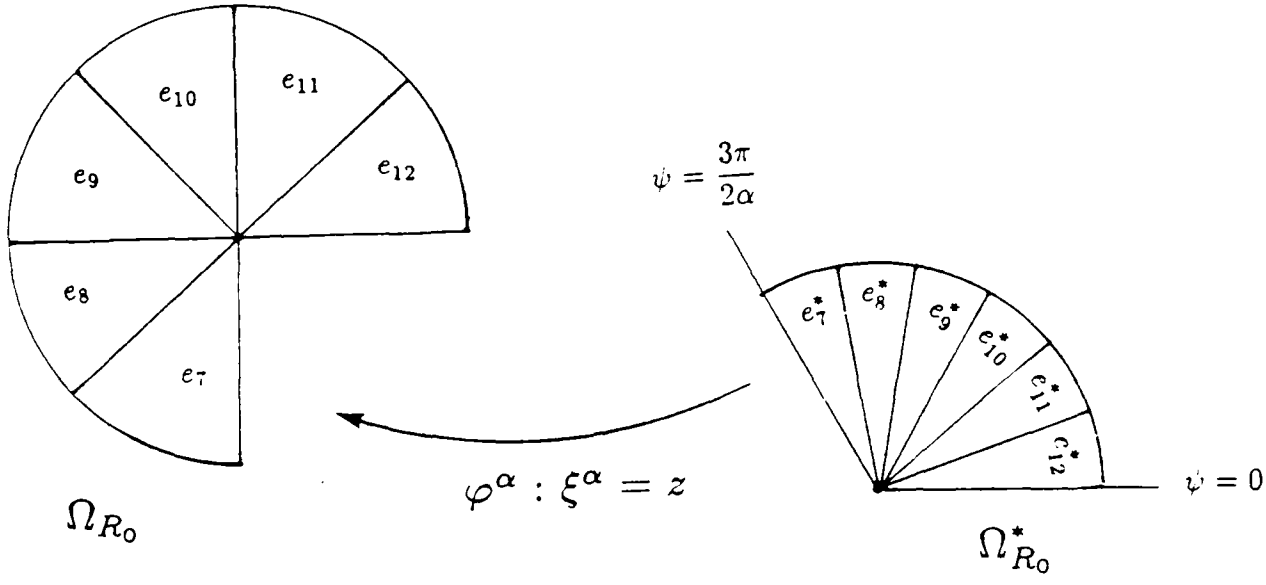

Figure 4.1.The Scheme of Ω_{R_0} and $\Omega_{R_0}^*$.

TABLE 4.1. The Relative Error for $\alpha = m(\frac{3}{2}), m = 2/3, 1, 2, 4$ when $f = 0$.

p \ α	1	$1\left(\frac{3}{2}\right)$	DOF
1	0.162846972467572D + 00	0.1176835578896779D + 00	10
2	0.6774829063879436D − 01	0.2709809653006089D − 01	32
3	0.4267764860979481D − 01	0.1392839460138052D − 01	60
4	0.2930203635221640D − 01	0.4078061954970974D − 02	100
5	0.2236678198833828D − 01	0.1137579818794599D − 02	152
6	0.1794231933116408D − 01	0.3390584498845191D − 03	216
7	0.1486700458517911D − 01	0.9705280386932562D − 04	292
8	0.1261468544746016D − 01	0.2757048098466325D − 04	380

p \ α	$2\left(\frac{3}{2}\right)$	$4\left(\frac{3}{2}\right)$	DOF
1	0.2437842370603280D + 01	0.3913546088255135D + 00	10
2	0.2757060901917393D − 01	0.1304975484223534D + 00	32
3	0.1408437528088371D − 01	0.2328733675022739D − 01	60
4	0.4142402706997820D − 02	0.4295634650207781D − 02	100
5	0.1149455073984022D − 02	0.1237407887180692D − 02	152
6	0.3425494364421739D − 03	0.4100441132194179D − 03	216
7	0.9736221988286052D − 04	0.1428178128929969D − 03	292
8	0.2746260993089290D − 04	0.4942584844978042D − 04	380

Theorem 4.2.

$$\|u_p^\alpha - u_0\|_E \leq \frac{C}{N_p^{(2/3)\alpha}} \tag{4.4}$$

where C is independent of N_p .

In theorem 4.1 and 4.2 the constant C depends on α. We have seen it in Table 4.1 and Fig. 4.2, where the error when $m = 4$ was higher than that when $m = 1$.

To see more in details these effects, let us investigate the error of an approximation of $(x+1)^\alpha, x \in I = (-1, 1)$ by polynomials in $L_2(I)$- norm.

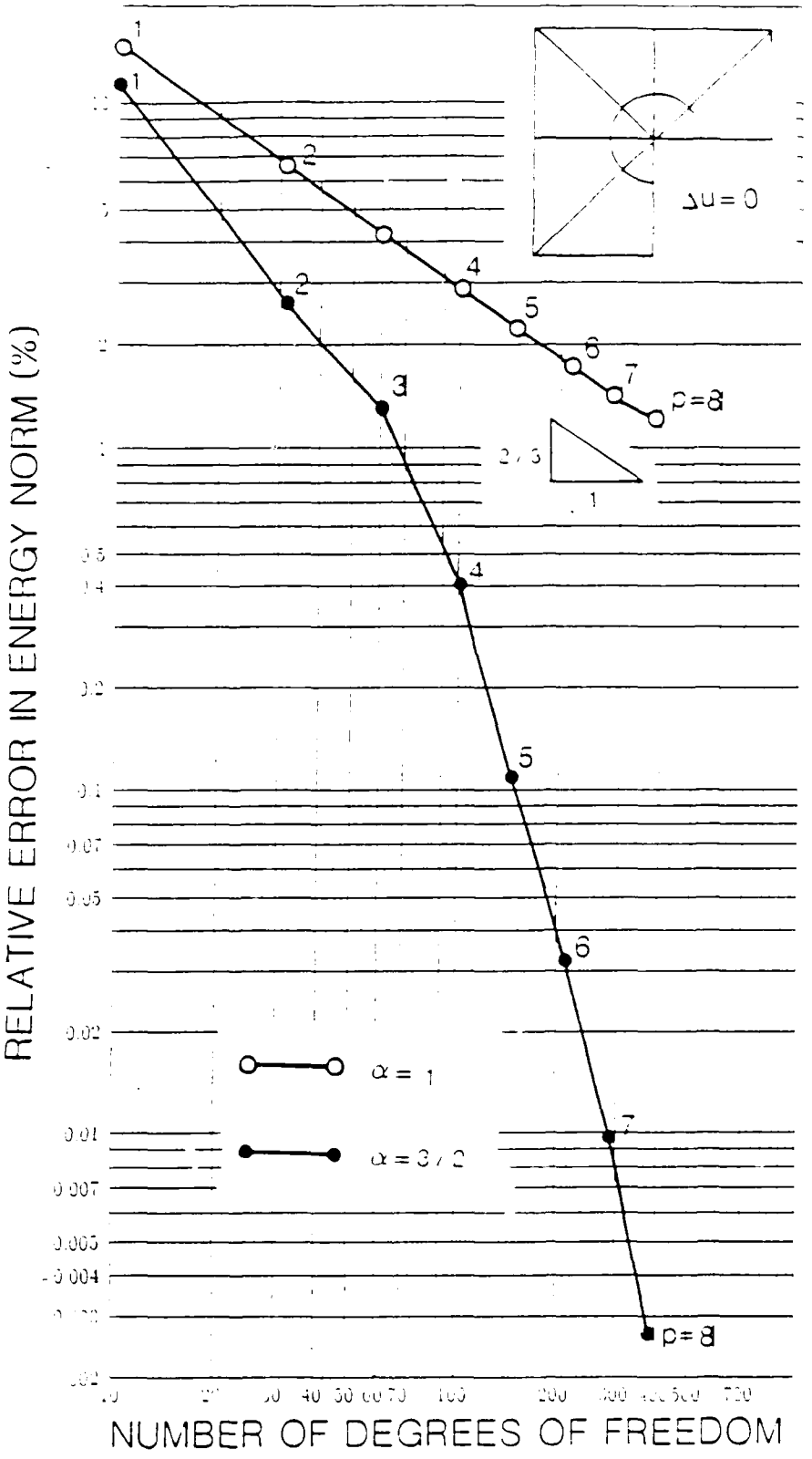

Fig. 4.2. The Relative Error in $\log \varepsilon \times \log N$ scale when $f = 0$.

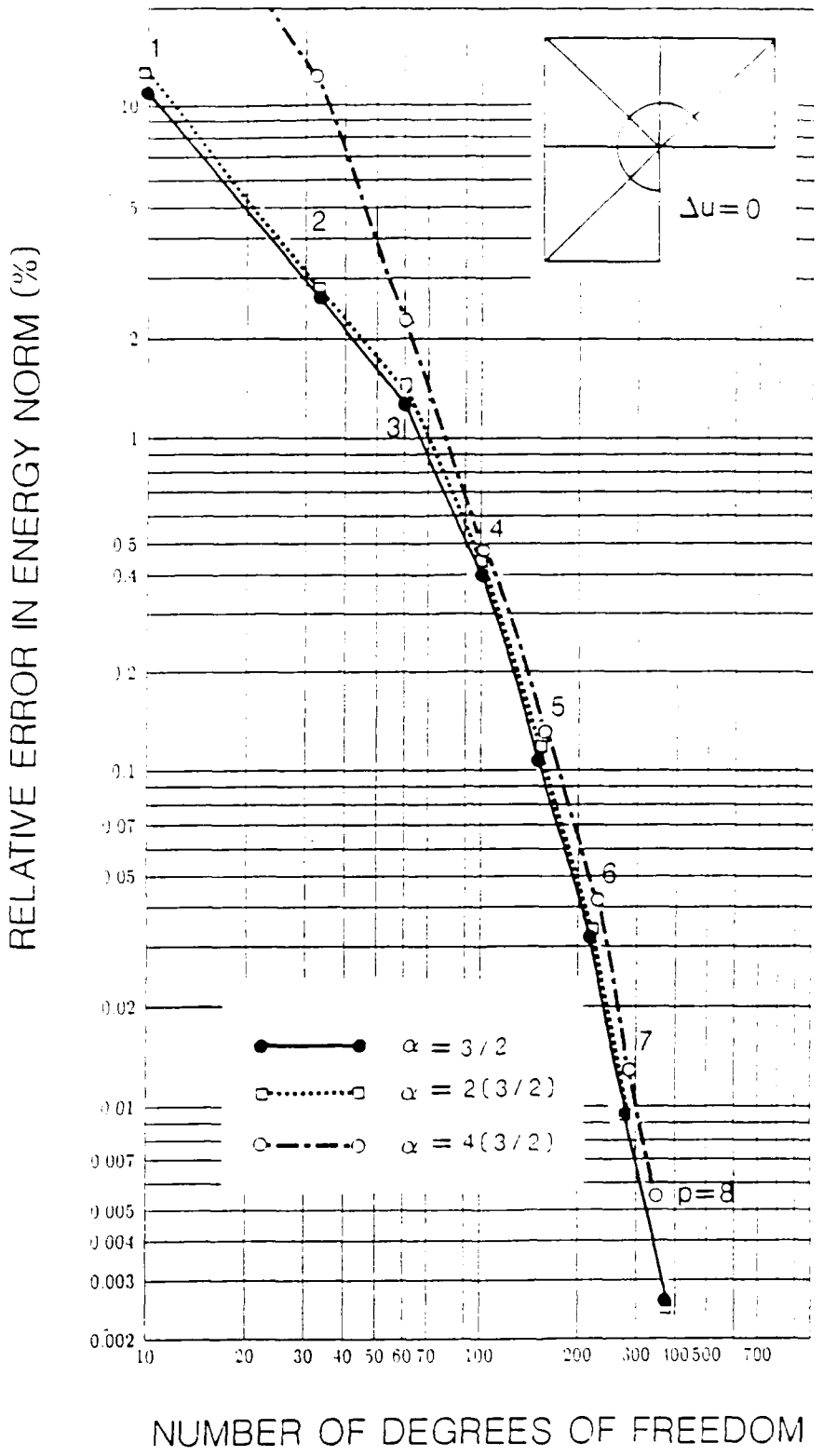

Fig. 4.3. The Relative Error for $\alpha = m(\frac{3}{2}), m = 1, 2, 4$ in $\log \varepsilon \times \log \mathcal{N}$ scale when $f = 0$.

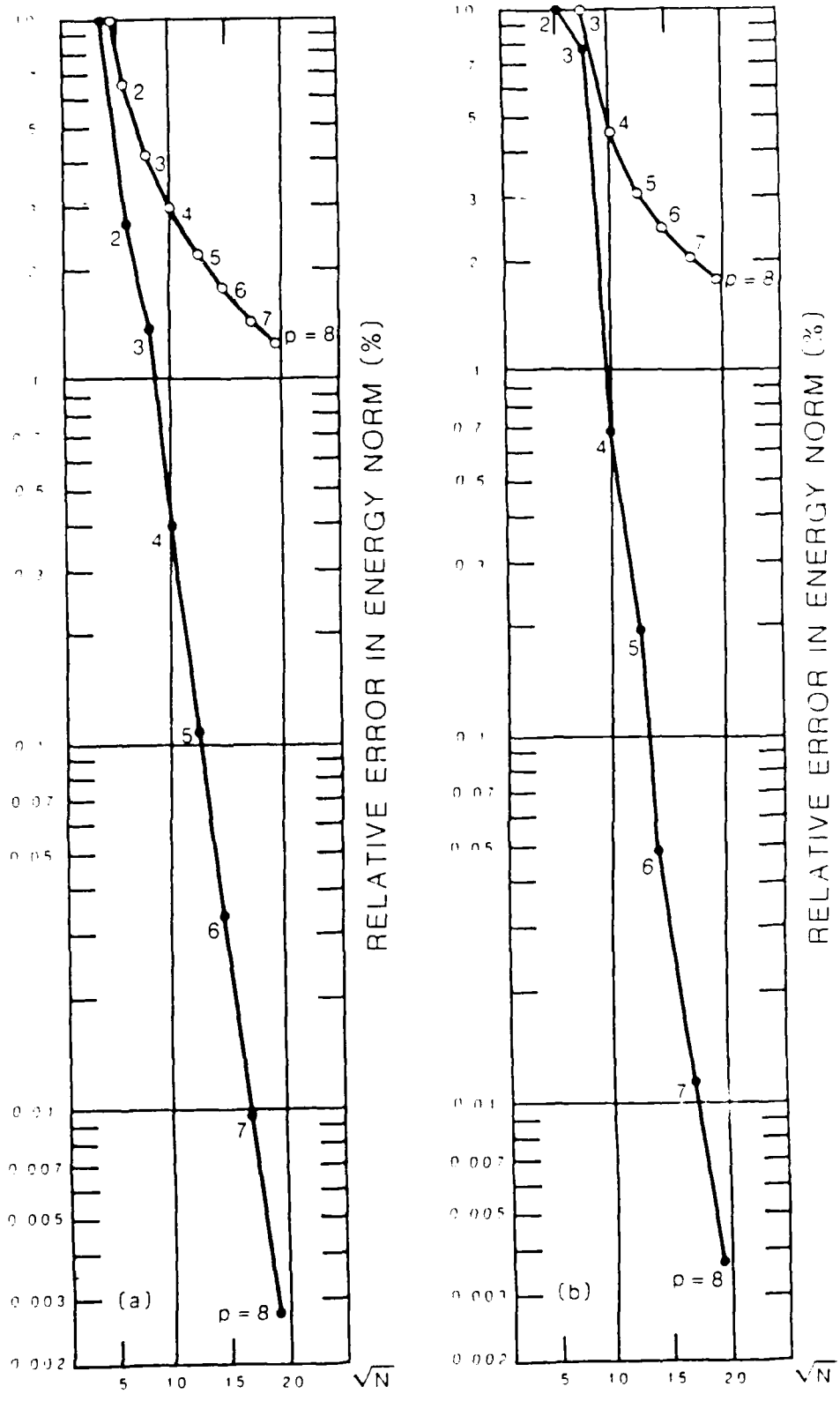

Fig.4.4. The Relative Errors in $\log \varepsilon \times \sqrt{N}$ scale (a) when $f = 0$ and (b) when $f = 1$ respectively.

From part 1 of [12], we have

Theorem 4.3.

$$\varepsilon_p = c_0(\alpha)\frac{2^{\alpha+1/2}}{(p+1)^{2\alpha+1}}(1+O(1/p)) \text{ as } p \to \infty \tag{4.5}$$

where

$$c_0(\alpha) = \frac{\Gamma(1+\alpha)^2|\sin\pi\alpha|}{(\sqrt{2\alpha+1})\pi}$$

The value $\alpha = 1/6$ gives the rate $\varepsilon_p = O(p^{-4/3})$ which is the same (in p) as in our example when no mapping is used. In the table 4.2 we give values of ϵ_p for some values of α and p when the term $(1+O(1/p))$ is neglected. We also give the values of the norm of $(x+1)^\alpha$ in $L_2(I)$ which is of course an upper bound of the error. We selected the value of α so that $|\sin\alpha\pi|$ has same value in the formula (4.5). We can see the typical behavior, that we have observed in Table 4.1, namely that for higher α the results are worse for low p (and low accuracy) while they are better for higher degree of polynomial(and higher accuracy). Hence in general the choice of α depends on the required accuracy.

In the above analysis, we have considered the mesh shown in Fig. 3.1. We can of course use the meshes with concentric layers which are used in the h-p version too (see Fig. 4.5) and use the mapping as before. By this we can combine mesh refinement approach and the auxiliary mapping technique.

So far we have assumed that $f = 0$ and hence the solution in a neighborhood of the corner can be expressed by the series (4.1). On the other hand, if $f \neq 0, f \in H^s(\Omega)$ then (4.1) is no longer true and the solution u_0 in Ω_{R_0} can now be written in the form(see,[19])

$$u_0(r,\theta) = \sum_{k=0}^{n} a_k r^{(\frac{2}{3})k}\sin(2/3)k\theta + \sum_{k=1}^{n/3} b_k r^{2k}\log r\sin 2k\theta + v(r,\theta), \tag{4.6}$$

where $v \in H^{s+2}(\Omega_{R_0})$, provided that $(2/3)(n+1) > s+1$.

Let us consider $f = 1$, then first term in the expansion of v is $r^2 \log r \sin 2k\theta$ and hence in contrast to the previous case we can not achieve (in general) an exponential rate of convergence even when f is analytic, but we can only have the rate $N_p^{-2\alpha} \log N_p$ ([8],[9]). In general we expect that the positive effect by the auxiliary mapping technique will be slightly smaller for $f \neq 0$ than for $f = 0$. Table 4.3 shows the errors for the mapping when $\alpha = m(\frac{3}{2})$, $m = 2/3, 1, 2$, and 4, and $m = 2/3$ stands for the case when no mapping technique was used . Fig. 4.6, 4.4(b) show the behavior of the error in the $\log \varepsilon \times \log N$ scale and $\log \varepsilon \times \sqrt{N}$ respectively. We actually see the differences as predicted. We see that the auxiliary mapping technique improves the accuracy very much when the degree of polynomial is ≥ 4.

So far we have used only one mapping. We can of course enrich the space $S(e)$ of elemental shape functions by functions stemming from identity mapping, i.e. by the usual shape functions. We can also add analogous shape functions using the conformal mapping $\xi = z^\beta \log z$. By such an enrichment we can once more achieve that the rate of convergence is exponential provided that f is analytic in $\hat{\Omega}$. Of course the complexity in computation now is higher and practical questions arise. However in contrast to the classical enrichment approach one advantage of this is that it does not violate the finite element architecture(in the implementation we add only internal shape functions of special type constructed by the mapping procedure).

As we mentioned above selecting the particular α properly and using higher degree of polynomials yields high accuracy. Let us also state that we can use high degree of polynomial only in the elements with vertex at the corners (in our example, elements 7-12) while keeping a low degree of polynomials in all other elements. A combination with mesh refinement procedure is also a valuable alternative especially because of the easiness of computing the local stiffness matrices.

TABLE 4.2. The error ε_p and the L_2-norm $\|u\|$ of $u = (1+x)^\alpha$ on I for $\alpha = (n + 1/6)$ and $(n + 5/6), n = 0, 1, 2, 3, 4.$

p \ α	$\frac{1}{6}$	$\frac{5}{6}$	$\frac{7}{6}$	$\frac{11}{6}$	$\frac{13}{6}$
1	7.4731D − 2	3.4188D − 2	3.2166D − 2	4.3432D − 2	5.9688D − 2
2	4.3522D − 2	1.1596D − 2	8.3258D − 3	6.5471D − 3	6.8665D − 3
3	2.9657D − 2	5.3843D − 3	3.1913D − 3	1.7100D − 3	1.4805D − 3
4	2.2025D − 2	2.9696D − 3	1.5168D − 3	6.0361D − 4	4.5034D − 4
5	1.7272D − 2	1.8262D − 3	8.2602D − 4	2.5778D − 4	1.7031D − 4
6	1.4063D − 2	1.2107D − 3	4.9412D − 4	1.2555D − 4	7.4850D − 5
7	1.1769D − 2	8.4798D − 4	3.1661D − 4	6.7328D − 5	3.6720D − 5
8	1.0059D − 2	6.1941D − 4	2.1381D − 4	3.8859D − 5	1.9592D − 5
9	8.7406D − 3	4.6769D − 4	1.5049D − 4	2.3766D − 5	1.1170D − 5
10	7.6975D − 3	3.6272D − 4	1.0953D − 4	1.5233D − 5	6.7187D − 6
11	6.8543D − 3	2.8761D − 4	8.1951D − 5	1.0149D − 5	4.2242D − 6
12	6.1605D − 3	2.3233D − 4	6.2760D − 5	6.9858D − 6	2.7565D − 6
13	5.5809D − 3	1.9067D − 4	4.9023D − 5	4.9433D − 6	1.8565D − 6
14	5.0904D − 3	1.5863D − 4	3.8951D − 5	3.5825D − 6	1.2850D − 6
15	4.6707D − 3	1.3355D − 4	3.1412D − 5	2.6509D − 6	9.1077D − 7
$\|u\|$	1.3747D + 0	1.5431D + 0	3.0238D + 0	2.3329D + 0	2.7495D + 0

p \ α	$\frac{17}{6}$	$\frac{19}{6}$	$\frac{23}{6}$	$\frac{25}{6}$	$\frac{29}{6}$
1	1.4586D − 1	2.5522D − 1	9.3989D − 1	1.9638D + 0	9.8958D + 0
2	9.7720D − 3	1.3049D − 2	2.7987D − 2	4.4624D − 2	1.3096D − 1
3	1.4357D − 3	1.5826D − 3	2.3129D − 3	3.0442D − 3	6.0879D − 3
4	3.2433D − 4	3.0810D − 4	3.3440D − 4	3.7930D − 4	5.6332D − 4
5	9.6187D − 5	8.0914D − 5	6.8870D − 5	6.9177D − 5	8.0567D − 5
6	3.4420D − 5	2.6126D − 5	1.8105D − 5	1.6411D − 5	1.5562D − 5
7	1.4132D − 5	9.8131D − 6	5.6915D − 6	4.7192D − 6	3.7452D − 6
8	6.4443D − 6	4.1370D − 6	2.0507D − 6	1.5720D − 6	1.0662D − 6
9	3.1925D − 6	1.9104D − 6	8.2288D − 7	5.8800D − 7	3.4655D − 7
10	1.6911D − 6	9.4970D − 7	3.6025D − 7	2.4157D − 7	1.2539D − 7
11	9.4678D − 7	5.0173D − 7	1.6947D − 7	1.0724D − 7	4.9565D − 8
12	5.5527D − 7	2.7896D − 7	8.4689D − 8	5.0804D − 8	2.1105D − 8
13	3.3880D − 7	1.6200D − 7	4.4555D − 8	2.5440D − 8	9.5736D − 9
14	2.1389D − 7	9.7678D − 8	2.4503D − 8	1.3361D − 8	4.4863D − 9
15	1.3910D − 7	6.0849D − 8	1.4005D − 8	7.3156D − 9	2.3041D − 9
$\|u\|$	3.9037D + 0	4.6895D + 0	6.8476D + 0	8.3136D + 0	1.2344D + 1

TABLE 4.3. The Relative Errors in Energy Norm for $\alpha = m(3/2), m = 2/3, 1, 2, 4$ when $f = 1$.

p \ α	1	$1\left(\frac{3}{2}\right)$	DOF
1	0.6020654757148309D + 00	0.5706890379221034D + 00	10
2	0.1308957854381257D + 00	0.1009916680045339D + 00	32
3	0.9925866863851720D − 01	0.8092169418184365D − 01	60
4	0.4203366119963193D − 01	0.6942004795074728D − 02	100
5	0.3198798981482650D − 01	0.2059652008864891D − 02	152
6	0.2563898916834782D − 01	0.5410328220679518D − 03	216
7	0.2124137148103968D − 01	0.1410620291464109D − 03	292
8	0.1802105654621925D − 01	0.3647987063804444D − 04	380

p \ α	$2\left(\frac{3}{2}\right)$	$4\left(\frac{3}{2}\right)$	DOF
1	0.6140576157783938D + 00	0.7227916745356786D + 00	10
2	0.1153904981172256D + 00	0.1685768303941887D + 00	32
3	0.8432233140432240D − 01	0.9410470781118301D − 01	60
4	0.8046799392682128D − 02	0.2885998162978118D − 01	100
5	0.2159258500150655D − 02	0.1095935137932326D − 01	152
6	0.5484874342364825D − 03	0.3570789379357526D − 02	216
7	0.1413509051434937D − 03	0.1052197244808133D − 02	292
8	0.3612904449632896D − 04	0.3077579620346113D − 03	380

Finally let us remark that if $f \neq 0$ then the computation of the elemental load vector is influenced by the auxiliary mapping. For example, if the conformal mapping $\varphi^\alpha : \xi^\alpha = z$ was used as in example 3.1 then

$$\tilde{f} = |J(\varphi^\alpha)|\hat{f} = \alpha^2 \rho^{2(\alpha-1)}(f \circ \varphi^\alpha)$$

has to be used for the elemental load vectors on the elements in $\Omega^*_{R_0}$.

In this section we are concerned only with the corner singularities, but our idea can be extended to deal with some other types of singularity as well. For example, the boundary singularity, known as the problem of Motz in the literatures(see [20], [25], [27]), can also

be treated very efficiently by using an argument similar to that given in this section. It will be elaborated elsewhere.

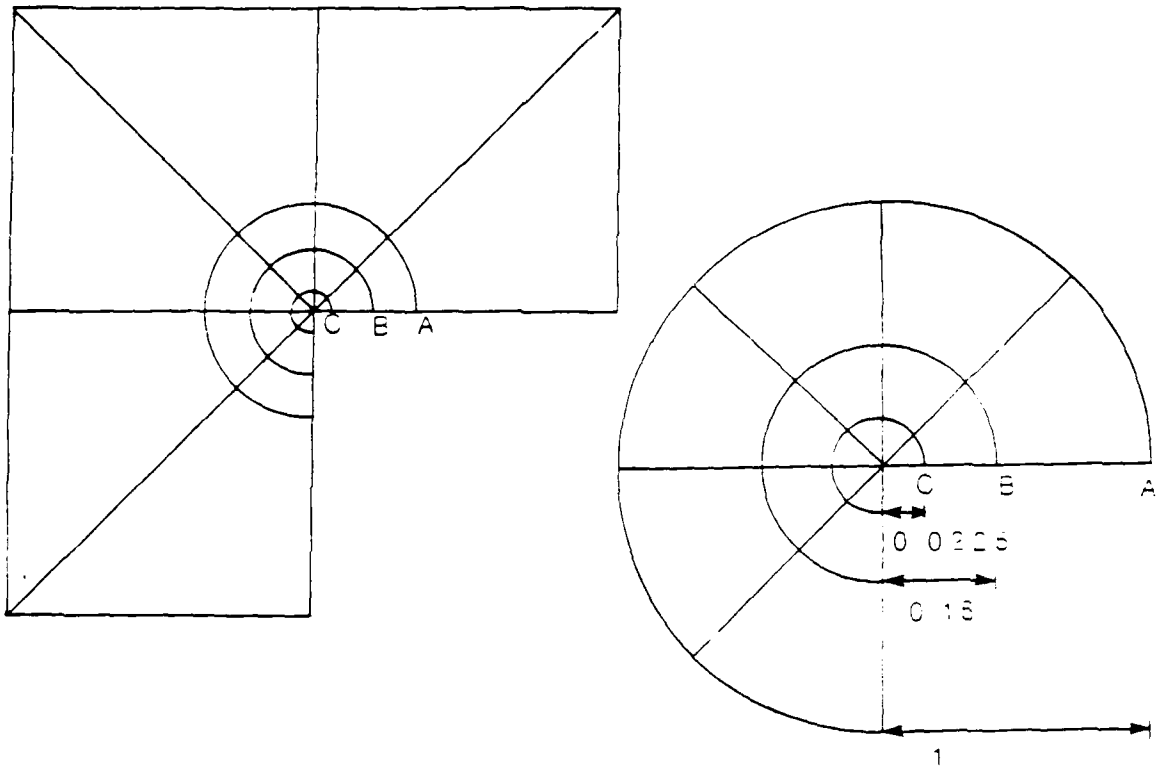

Figure 4.5. The Refined Mesh on the L-Shaped Domain Ω for the h-p Version.

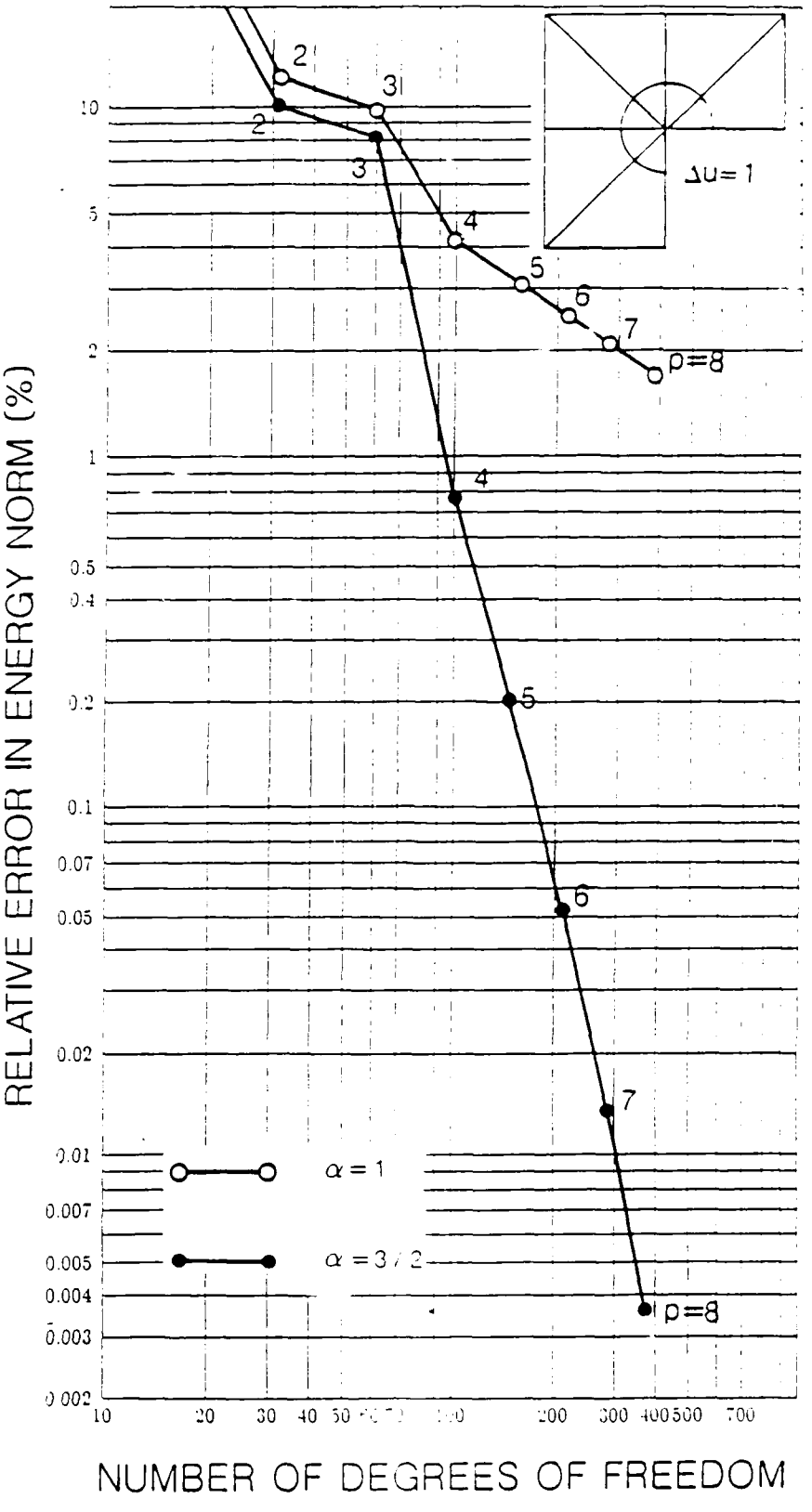

Figure 4.6. The Relative Error in $\log \epsilon \times \log N$ scale when $f = 1$.

5. The Method of Auxiliary Mapping for the General Elliptic Differential Equation of Second Order.

In the previous sections, we have applied the auxiliary mapping technique to the Laplace operator. In this section we will show that this technique can also be used for general elliptic boundary value problems. In the case of Laplace operator, Corollary 2.1 guarantees the simpleness of computing the elemental stiffness matrices. However in the case of general elliptic operator we need to use lemma 2.1 for computing elemental stiffness matrices and hence the routines for differential equations with nonconstant coefficients should be used for the computation in general. Even if the given problem has constant coefficients, the coefficients we are concerned in the auxiliary mapping technique are polynomials in $\sin x$ and $\cos x$. This fact has to be taken in account because quadrature formula are used in the computation of the stiffness matrices. Nevertheless they lead to uniformly elliptic operator. Hence for $f = 0$ one can achieve once again the exponential rate of convergence as before. Similar situation also occurs for $f \neq 0$.

We now describe the mapping technique for the general case with the mesh shown in Fig. 3.1. This goes as follows:

(Step a) Select parameter α for the mapping φ^α

(Step b) Map elements $e_7, ..., e_{12}$ onto $e_7^*, ..., e_{12}^*$ by the mapping $(\varphi^\alpha)^{-1}$ and construct the coefficients of the transformed elliptic operator and bilinear form: Since $(\varphi^\alpha)^{-1}(z) = z^{1/\alpha}$ we have

$$M = \begin{bmatrix} \cos(1-\alpha)\psi & -\sin(1-\alpha)\psi \\ \sin(1-\alpha)\psi & \cos(1-\alpha)\psi \end{bmatrix}$$

and by lemma 2.1 the coefficient q_{ij} of the transformed elliptic operator can be computed by the following formula

$$(5.1) \qquad \begin{cases} t = (1-\alpha)\psi \\ q_{11} = \hat{a}_{11}\cos^2 t + \hat{a}_{22}\sin^2 t - (\hat{a}_{21} + \hat{a}_{12})\sin t \cos t \\ q_{12} = (\hat{a}_{11} - \hat{a}_{22})\sin t \cos t - \hat{a}_{21}\sin^2 t + \hat{a}_{12}\cos^2 t \\ q_{21} = (\hat{a}_{11} - \hat{a}_{22})\sin t \cos t - \hat{a}_{12}\sin^2 t + \hat{a}_{21}\cos^2 t \\ q_{22} = \hat{a}_{11}\sin^2 t + \hat{a}_{22}\cos^2 t + (\hat{a}_{12} + \hat{a}_{21})\sin t \cos t \end{cases}$$

where $\hat{a}_{ij} = a_{ij} \circ \varphi^{\alpha}$ and (ρ, ψ) is the polar coordiates in the ξ-plane.

(Step c) Taking care of numerical integration, compute the elemental stiffness matrix on e_j^* with the coefficients $q_{ij}(\xi)$ and the elemental load vector on e_j^* with the right hand side $\tilde{f} = (\alpha^2 \rho^{2(\alpha-1)}) \cdot (\hat{f}(\rho, \psi))$

(Step d) Determine the finite element solution u_{FE} by solving the assembled global system. The solution at a point $x \in e_j$ can be obtained by evaluating the solution on e_j^* at $\xi_x = (\varphi^{\alpha})^{-1}(x)$.

It is worth to note the following observation about the case when the coefficient a_{ij} are constants: suppose λ_1 and λ_2 are the eigenvalues of the symmetric matrix $A = [a_{ij}]$ then there is an orthogonal matrix P such that $PAP^T = \text{diag}\,(\lambda_1, \lambda_2)$. If Ψ denotes the mapping defined by

$$\Psi(x, y) = (\frac{1}{\sqrt{\lambda_1}} x, \frac{1}{\sqrt{\lambda_2}} y)$$

then Ψ maps the elliptic subdomain

$$K = \{(x, y) : \frac{x^2}{\lambda_1} + \frac{y^2}{\lambda_2} \leq 1\} \cap \Omega$$

onto the circular subdomain $\Omega_{R_0} = \{z : |z| \leq 1\} \cap \Omega$. Let us denote $P^{-1}(K)$ and $(\varphi^{\alpha})^{-1}(\Omega_{R_0})$ by $\tilde{K}$ and $\Omega_{R_0}^*$ respectively. That is,

$$\tilde{K} \xrightarrow{P} K \xrightarrow{\Psi} \Omega_{R_0} \xrightarrow{(\varphi^{\alpha})^{-1}} \Omega_{R_0}^*.$$

Then by an argument similar to that of lemma 2.1 we have

$$\iint_{\tilde{K}} (\nabla u) \cdot A \cdot (\nabla v)^T dx = \sqrt{\lambda_1 \lambda_2} \iint_{\Omega_{R_0}^*} \nabla \hat{u} \cdot \nabla \hat{v} d\xi \tag{5.2}$$

In particular, if $a_{12} = a_{21} = 0$, we have

$$\iint_K (a_{11}\frac{\partial u}{\partial x_1}\frac{\partial v}{\partial x_1} + a_{22}\frac{\partial u}{\partial x_2}\frac{\partial v}{\partial x_2})dx = \sqrt{a_{11}a_{22}} \iint_{\Omega^*_{R_0}} \nabla\hat{u}\cdot\nabla\hat{v}d\xi \tag{5.3}$$

and the computation of elemental stiffness matrix and load vector on e^* in $\Omega^*_{R_0}$ is as simple as the case of Laplace operator. We can also use here the triangular elements with elliptic arcs which are allowed in PROBE. The mapping Technique together with this observation is leading to another approach to deal with interface singularities. Detailed argument of this will be presented elsewhere.

In similar way, we can treat the plane elasticity problem. For example, in the case of crack where the sides are not loaded the solution has a simple form and the auxiliary mapping technique with the conformal mapping $z = \xi^\alpha$ will lead to the rate $N_p^{-\alpha}$ of convergence analogously as before. Unfortunately in contrast to the case of the Laplace operator the local stiffness matrices has to be computed via nonconstant coefficients of the form similar to (5.1).

6. Elliptic Problems on Unbounded Domains.

In a similar manner to the previous sections the method of auxiliary mappings can deal the problems on unbounded domains. Let us address this with a model problem on an unbounded domain Ω with bounded boundary Γ (this is , Ω is the outside of a bounded domain enclosed by a simple closed curve Γ).

$$-\Delta u = f \quad \text{in } \Omega, \tag{6.1a}$$

$$u = 0 \quad \text{on } \Gamma_D, \tag{6.1b}$$

$$\frac{\partial u}{\partial n} = g \quad \text{on } \Gamma_N, \tag{6.1c}$$

where Γ_D and Γ_N are unions of analytic arcs as section 3 and Γ is a simple closed curve. For simplicity we will assume that $\Gamma_D \neq 0$ and the orgin is inside of Γ.

Let Ψ be the conformal mapping $\xi = \frac{1}{z}$, and let

$$W^1(\Omega, \Psi) = \{u \in L_c(\Omega) : (\iint u^2 |J(\Phi)| + \iint \nabla u \cdot \nabla u) < \infty\},$$

$$W_D^1(\Omega) = \{u \in W^1(\Omega, \Psi) : u = 0 \text{ on } \Gamma_D\}$$

Suppose

$$\iint_\Omega |f|^2 \frac{1}{|J(\Psi)|} < \infty,$$

then there exists a unigue $u \in W_D^1(\Omega)$ such that

$$\iint_\Omega \nabla u \cdot \nabla v dx = \iint_\Omega f v dx + \int_{\Gamma_N} g v ds, \text{ for all } v \in W_D^1(\Omega)$$

Suppose the mesh on Ω is as shown in Fig. 6.1. Then by the conformal mapping Ψ the infinite elements e_j^∞ will be mapped to the curvilinear trangular elements e_j^*. Now we can proceed as before. For example, suppose $f = 0$ and on $\Gamma = \partial\Omega$ we prescribed the same boundary conditions as section 3 and the mesh on Ω is as shown in Fig. 6.1. Then combining the auxiliary mapping technigue in the neighborhood of every vertex and the auxiliary mapping Ψ for the infinite elements we can achieve an exponential rate of convergence as before, i.e.

$$\|u_0 - u_p\|_{W^1(\Omega,\Psi)} \leq Ce^{-\gamma\sqrt{N_p}}$$

Let us show one numerical example.

Example 6.1. Let us consider Laplace's equation on $\Omega = \{z : |z| \geq 1/2\}$. Suppose $\Omega_{R_0} = \{z : |z| \leq 1\}$, the mesh is as shown in Fig. 6.2. and we impose the nonhomogeneous Dirichret boundary condition on Γ by the true solution $u(x, y) = x/(x^2 + y^2)$. Then

the relative error in energy norm is as shown in Table 6.1 and we can see once again the exponential rate of convergence in Fig. 6.3.

Table 6.1. The Total Strain Energy and The Relative Error for Laplace's Equation on the Unbounded Domain.

p	Total Energy	Relative Error in Energy Norm	DOF
1	11.16236197243942	0.3342565747335926D + 00	9
2	12.43592792490380	0.1018837543895582D + 00	29
3	12.56842346856016	0.1278127328426342D − 01	53
4	12.56658836901951	0.4162735313104689D − 02	89
5	12.56637844630835	0.7894597600800805D − 03	137
6	12.56637082991567	0.1309711457162764D − 03	189
7	12.56637061959958	0.2042102697231802D − 04	269
8	12.56637061447803	0.3075441953279617D − 05	353

Similar approach can also be applied for the conformal mapping $\xi = 1/(z^{\alpha})$ and also for the general differential equation and elasticity problems. It is essential that the solution has finite energy and that we consider the behaviour of the solution at ∞. So far we mentioned only the case when the boundary is bounded only. By the same approach we can deal with infinite domains such as half plane etc. We memtion that the implemention of the infinite elements is exactly as simple as for ther finite elements we disscused in previous sections. Many times we are dealing with the case that the solution does not belong to the space $H^1(\Omega)$ because of the behavour at ∞. Typical case is when on the bounadry Γ we prescribed the following singular boundary condition:

$$\frac{\partial u}{\partial n} = g, \qquad \int_{\Gamma} g ds \neq 0 \quad \text{and } f = 0.$$

Then the solution at ∞ is of form $u \approx C \log r$ and we have to enrich the space of elemental shape functions by this function analoguously as we disscussed earlier. Of course we have to adjust the approach to the fact that we deal with one shape function with infinite energy. This can be dealt in different manner.

7. Conclusion

The h-p version allows a very effective and simple treatment of the singularities of the solution caused by the corners of domains and by the unboundedness of domains in R^2. This approach can be combined with elemental enrichment procedure and the mesh refinement procedure.

By using this approach one can obtain a higher rate of convergence in almost all applications. From the view-point of implementation, the easiest and the cheapest approach is **the auxiliary mapping technique** with possibly nonunifom polynomial degrees over the elements.

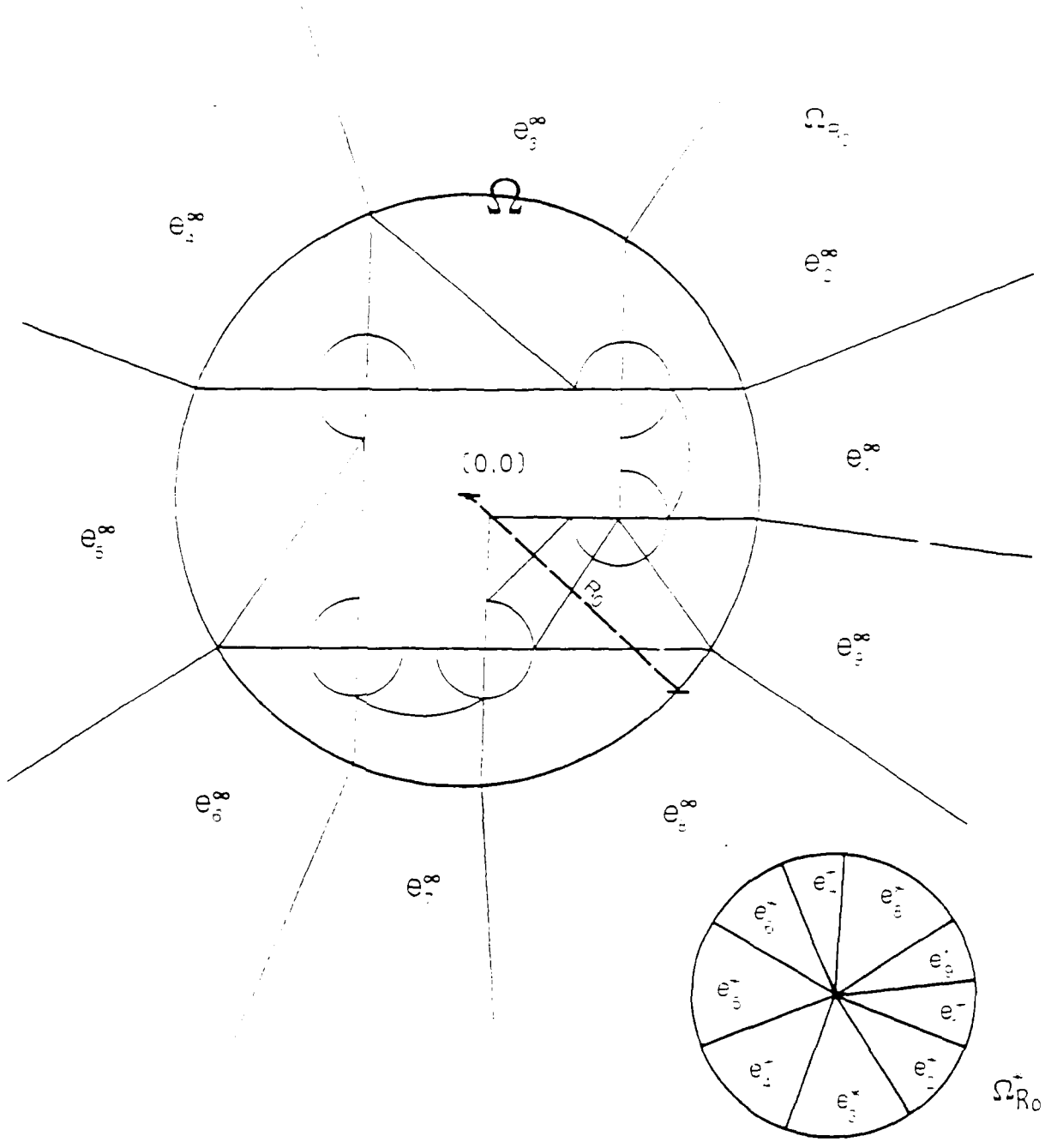

Fig 6.1. Mesh on the Exterior of an L-Shaped Domain for the Auxiliary Mapping Technique.

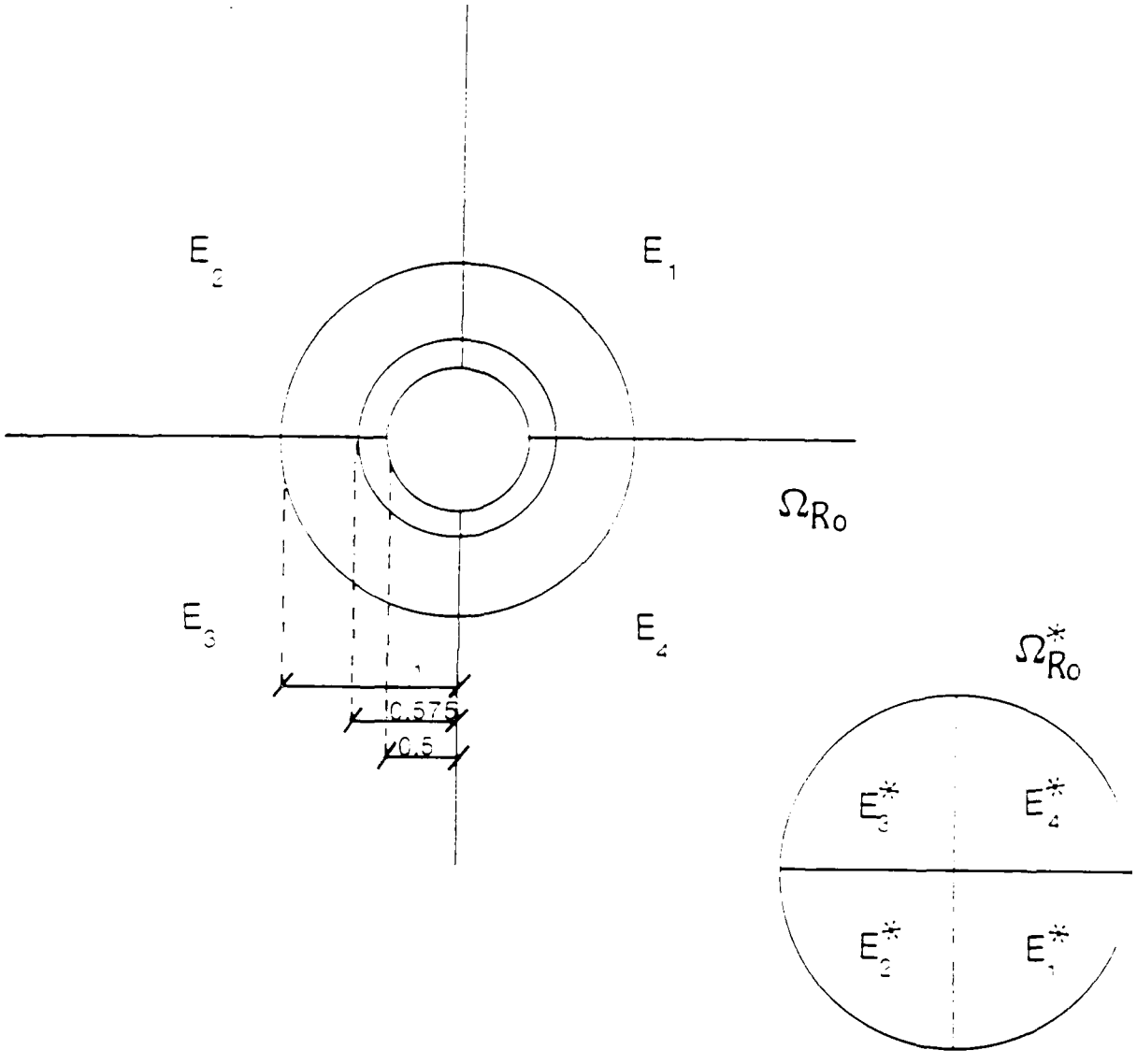

Fig. 6.2. The Scheme of the Infinite Domain Ω and a Bounded Subdomain Ω_{R_0}.

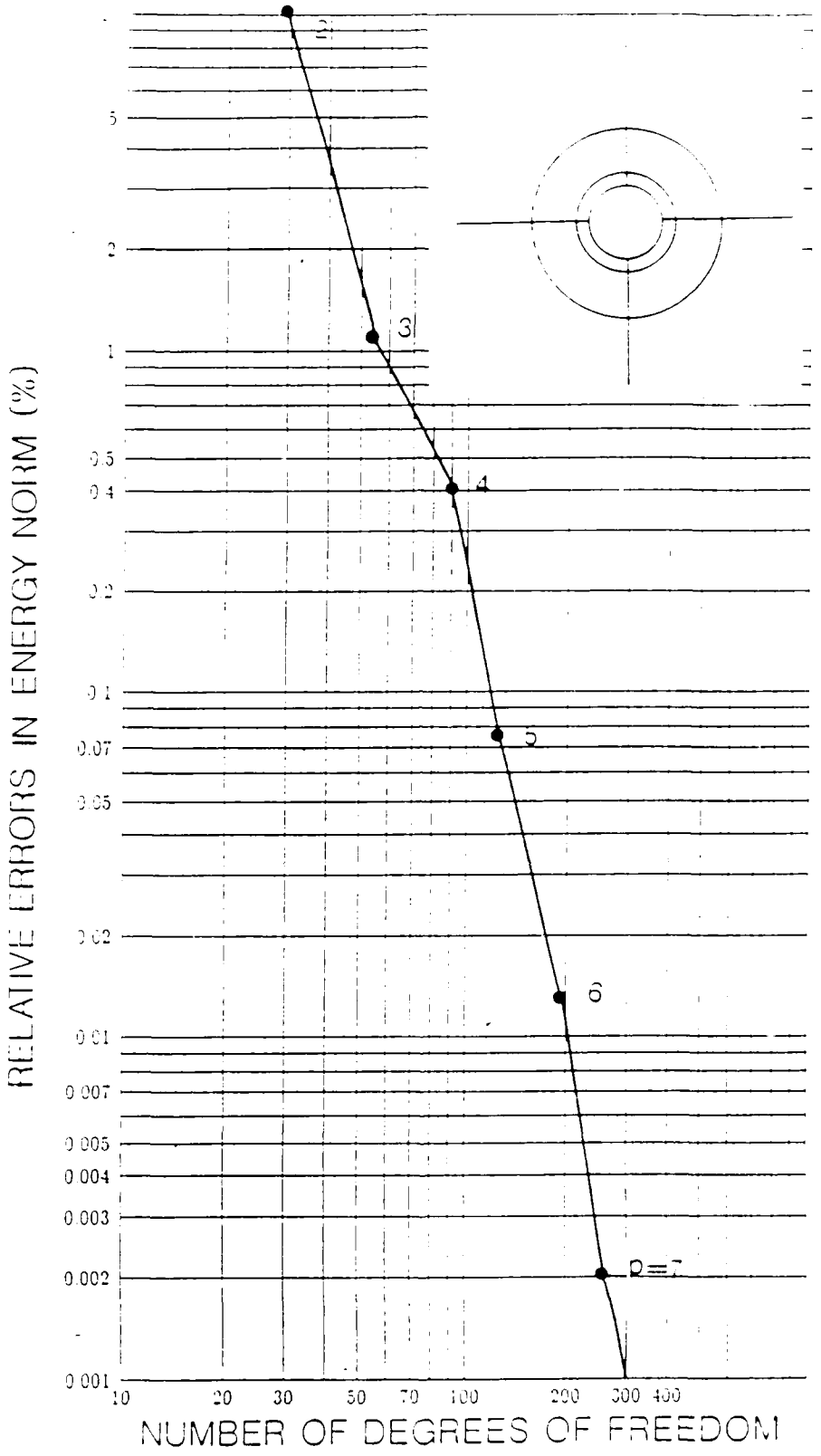

Fig. 6.3. The Relative Error of Laplace's equation on Infinite Domain in $\log \varepsilon \times \log N$ scale.

REFERENCES

[1] Akin, J. E. :*The Generation of Elements with Singularities,* Int. J. Numer. Meth. Eng., v. 10, 1976, pp.1249-1259.

[2] Akin, J. E. :*Elements for the Analysis of Line Singularities,* The Mathematics of Finite Elements with Applications, v. 3, ed. J.R. Whiteman, Academic Press, London, 1979.

[3] Babuška, I. : *The Finite Element Method for Infinite Domains,I* , Math. Comp. ,v. 36, 1972, pp. 1-11.

[4] Babuška, I. and Guo, B. : *The h-p Version of the Finite Element Method For Domains with Curved Boundaries,* SIAM J. Numer. Anal., V.25, 1988, pp. 837-861

[5] Babuška, I. and Guo, B. : *Regualrity of the Solutions of Elliptic Problem with Piecewise Analytic data, part I: Boundary Value Problems for linear Elliptic Equation of Second Order,* SIAM J. Math. Anal., v. 19, 1988, pp.172-203.

[6] Babuška, I. ,Kellogg, B. and Pitkäranta, J.: *Direct and Inverse Error Estimates for Finite Elements with Mesh Refinements,* Numer. Math. v. 33, 1979, pp. 447-471.

[7] Babuška, I. and Rosenzweig, M. R. :*A Finite Element Scheme for Domains with Corners,* Numer. Math. v. 20, 1972, pp. 1-21.

[8] Babuška, I. and Suri, M. :*The Opitimal Convergence Rate of the p-Version of the Finite Element Method,* SIAM J. Numer. Anal. v. 24, No. 4 ,1987, pp. 750-776.

[9] Babuška, I. and Suri, M. :*The h-p Version of the Finite Element Method with Quasi-uniform Meshes,* IPST, Univ. of MD. Technical Note BN-1046, April ,1986.

[10] Babuška, I., Szabo, B. A. and Katz, I. N. : *The p-Version of the Finite Element Method* , SIAM J. Numer. Anal. v. 18, 1981, pp. 515-545.

[11] Ciarlet, P. G. :*The Finite Element Method for Elliptic Problems,* North-Holland, Amsterdam, 1978.

[12] Gui, W. and Babuška, I. : *The h-p Versions of the Finite Element Method in One Dimension. Part 1: the Error Analysis of the p-Version; Part 2: the Error Analysis of the h and h-p Versions; Part 3: the Adaptive h-p Version*, Numer. Math., v. 49, 1986, pp. 577-683.

[13] Guo, B. and Babuška, I. : *The h-p Version of the Finite Element Method. Part 1: The basic Application Results*, v. 1, 1986, pp. 21-41.

[14] Guo, B. and Babuška, I. : *The h-p Version of the Finite Element Method. Part 2: General Results and Applications*, v. 1, 1986, pp. 203-220.

[15] Goldstein, C. I. :*The Finite Element Method with Nonuniform Mesh Sizes for Unbounded Domains*, Math. Comp., v. 36, 1981, pp. 387-404.

[16] Fix, G., Gulati, S. and Wakoff, G. I. : *On the Use of Singular Functions with the Finite Element Method,* J. of Comp. Physics , v. 13, 1973, pp. 209-228.

[17] Han, H. D. and Wu, X. N. : *Approximation of Infinite Boundary Condition and its Application to the Finite Element Method* , J. Comp. Math., v. 3, 1985, pp. 179-182.

[18] Johnson, C. and Nedelec, J. C. : *Coupling of Boundary Integral and Finite Element Methods,* Math. Compt., v. 35, 1980, pp. 1063-1079.

[19] Kondrat'ev, V. A. :*Boundary Problems for Elliptic Equations with Conical or Angular Points,* Trans. Moscow Math. Soc., v. 16, 1967, pp. 227-313.

[20] Zi-Cai Li: *A nonconforming Combined Method for Solving Laplace's Boundary Value Problems with Singularities,* Numer. Math., v. 49, ,1986, pp. 475-497.

[21] Silvester, P. and Hsieh, M. S. : *Finite Element Solution of 2-Dimensional Exterior Field Problems,* Proc. IEE, v. 118, 1971, pp. 1743-1747.

[22] Stern, M. :*Families of Consistent Conforming Elements with Singular Derivative fields,*Int. J. Numer. Meth. Eng., v. 14 , 1979, pp. 409-421.

[23] Strang, G. and Fix, G. :*An Analysis of Finite Element Method,* Prenticw-Hall, 1973.

[24] Szabo, B. A. :*PROBE :* The Theoretical Manual(Release 1.0), Noetic Tech. Cor. St Louis, MO., 1985.

[25] R.W. Thatcher: *The Use of Infinite Grid Refinements at Singularities in the Solution of Laplace's Equation.* Numer. Math., v. 25, 1976, pp. 163-178.

[26] Tsamasphyros, G.:*Singular Element Construction Using a Mapping Technique,* Int. J. Numer Meth. Eng., v. 24, 1987, pp. 1305-1316.

[27] Witeman,J. R. and Papamichael, N.: *Treatment of Harmonic Mixed Boundary Problems by Conformal Transformation Methods*, ZAMP, v. 23, 1972, pp. 655-663.

[28] Zienkiewicz, O. C. ,Bando, K., Bettess, P., Emson, C. and Chiam, T. C.: *Mapping Infinite Elements for Exterior Wave Problems,* Int. J. Num. Method Eng., v. 21,1985, pp. 1229-1251.

[29] Zienkiewicz, O. C., Emson, C., Bettes, P. :*A Novel Boundary Infinite Element*, Int. J. Numer. Meth. Engrg. v. 19, 1983, pp. 393-404.

The Laboratory for Numerical analysis is an integral part of the Institute for Physical Science and Technology of the University of Maryland, under the general administration of the Director, Institute for Physical Science and Technology. It has the following goals:

- To conduct research in the mathematical theory and computational implementation of numerical analysis and related topics, with emphasis on the numerical treatment of linear and nonlinear differential equations and problems in linear and nonlinear algebra.

- To help bridge gaps between computational directions in engineering, physics, etc., and those in the mathematical community.

- To provide a limited consulting service in all areas of numerical mathematics to the University as a whole, and also to government agencies and industries in the State of Maryland and the Washington Metropolitan area.

- To assist with the education of numerical analysts, especially at the postdoctoral level, in conjunction with the Interdisciplinary Applied Mathematics Program and the programs of the Mathematics and Computer Science Departments. This includes active collaboration with government agencies such as the National Bureau of Standards.

- To be an international center of study and research for foreign students in numerical mathematics who are supported by foreign governments or exchange agencies (Fulbright, etc.)

Further information may be obtained from Professor I. Babuška, Chairman, Laboratory for Numerical Analysis, Institute for Physical Science and Technology, University of Maryland, College Park, Maryland 20742.